SCA2003-11: INTERPRETATION OF A LONG-CORE HEAVY OIL DEPLETION EXPERIMENT USING PORE NETWORK MODELLING TECHNIQUES

I. Bondino, S. R. McDougall, Heriot-Watt University and G. Hamon, Total

This paper was prepared for presentation at the International Symposium of the Society of Core Analysts held in Pau, France, 21-24 September 2003

ABSTRACT

The performance of a solution gas drive experiment is ultimately determined by a complex interaction of a variety of different petrophysical parameters, including the rate of pressure decline and the chemical and physical properties of the rock-fluid system itself (*viz:* the nucleation properties of the porous medium, the gas-oil diffusivity, oil viscosity, gas-oil interfacial tension, dissolved gas-oil ratio, pore connectivity, etc). Here, a pore-scale process simulator is used to interpret the underlying dynamic processes that characterise a long-core heavy oil depletion experiment. This is achieved by direct matching of experimental gas and oil production profiles under different depletion rates.

Progressive nucleation is implemented in the simulator, whereby bubbles nucleate from sites of increased "nucleation potential" — in keeping with recent developments in the field. The complex phenomenon of nucleation is discussed here in terms of the combined effects of (i) the spatial distribution of nucleation potential, (ii) depletion rate and (iii) the characteristics of the oil under investigation. Different bubble densities are produced at different depletion rates via a physically-based nucleation algorithm. As a result excellent history-matches of two heavy oil depressurisation experiments are obtained. The associated relative permeability curves are also presented.

Finally, close analysis of the simulation data also allows us to investigate the widely-held belief that recovery efficiency is directly linked to depressurisation rate — the higher the depletion rate, the larger the number of bubbles nucleated, and the higher the observed recovery. We show here that recovery is seen to depend not only upon the depletion rate and bubble density, but also upon the lengths of diffusion pathways, local supersaturation gradients, and gas cluster topology — all of which are related to the underlying connectivity of the pore system.

INTRODUCTION

In a conventional light oil depressurisation process, gas bubbles start to nucleate as the pressure is lowered below the bubble point pressure of the oil. These bubbles then grow (mainly by expansion and diffusion of light components from the liquid oil phase), coalesce, and, under certain circumstances, may migrate via buoyancy forces towards the top of the system. The precise manner in which this growing, migrating gas phase displaces oil from the porous matrix depends upon a number of experimental factors, including: the laboratory depletion rate, core orientation, positioning of production ports,

and overburden pressure. In addition, the chemical characteristics of the rock-hydrocarbon system itself play a crucial role (PVT parameters, interfacial tension, gas-oil diffusion coefficients, wettability), as do the physical characteristics of the porous medium (pore connectivity and topology). This paper attempts to elucidate how each of these factors affects gas evolution and oil recovery during depressurisation generally, and then goes on to apply this newly-acquired insight to a heavy oil depletion experiment.

It is a well-known fact that the depressurisation of a heavy oil is quite different from that of a conventional low viscosity oil. Heavy oils often show much better recoveries than expected, both in the field and under laboratory conditions. This is often thought to be due to a "foamy oil" flow regime, in which oil and microbubbles of dimensions much smaller than the pore size flow simultaneously through the rock interstices. Under field conditions, foamy oil formation and the associated enhanced recovery are thought to be caused by (i) geomechanical effects (sand production and the concomitant emergence of high permeability channels) and/or (ii) high pressure gradients in the near-well region [1,2]. In the laboratory, however, "foamy" behaviour would be due mainly to the high depressurisation rates that characterise core depletion experiments. Examples from the literature, from both core and micro-model experiments, show that foamy oil forms more readily when depletion rates and pressure gradients are increased. This produces viscous forces that are large enough to mobilize and break up isolated gas bubbles, with asphaltenes possibly playing a stabilising role by preventing subsequent coalescence [3,4,5,6].

In this work a heavy oil long core depletion experiment has been interpreted using pore network modelling. Microbubbles do not form in any great numbers and do not flow with their associated oil — in short, gas remains trapped in the pore matrix under capillary dominated growth conditions. Using this approach, experimental oil productivities at different laboratory depletion rates have been successfully matched and the associated relative permeability curves derived.

THE HEAVY OIL LONG-CORE EXPERIMENT: PRODUCTION PROFILES AND EXPERIMENTAL CONSIDERATIONS

Here we report the main features of the core depressurisation experiments that are pertinent to the simulation study — fluid and core properties are reported in Tables 1 and 2. More details are available in [7]. The core is vertically orientated and production takes place from the top of the sample. Cumulative gas and oil production for two depletion rates of 9 psi/day and 100 psi/day are reported in Figure 1. Production of a dissolved gas and oil starts at about 725 psi in both cases and gas breakthrough occurs at approximately 26 bars (377 psi) for the high rate case and approximately 42 bars (609 psi) in the lower rate. We assume that gas breakthrough is an indicator of critical gas saturation.

Past work with the depressurization network simulator [8] has shown that the greater the number of nucleated bubbles (as a result of a faster depletion rate), the slower their individual growth rate. This means that higher depletion rates lead to a delay in the

coalescence of individual gas clusters — this would explain the delayed gas breakthrough observed in the higher rate experiment. It can also be noticed that in the proximity of the gas breakthrough points (377psi high rate and 609psi low rate), the gas production rates increase and the oil production rates decrease. These experiments also show that a considerable amount of oil can still be produced beyond the stage at which gas becomes connected to the production port of the apparatus — this is especially evident in the low rate experiment. Furthermore the amounts of gas produced are similar at both depletion rates: hence, for these particular experiments, the mechanism by which oil is produced is independent of the overall amount of gas produced at the outlet — it appears that more gas remains trapped inside the core at the higher depletion rate.

In order to match the depletion experiments, we need a clear insight into the dynamics of gas evolution in a real rock, which can then be interpreted in the context of network model observations. Depletion experiments show that once free gas production becomes continuous, oil production starts decreasing. A number of comments/hypotheses can be made in light of this observation:

1) a continuous flow of gas means that an important gas cluster is now connected to the outlet.
2) the connected cluster no longer has any reason to grow preferentially “inside” the core, where capillary forces must be overcome; it simply flows out of the core: in other words growth of a gas cluster follows the path of least resistance once connected to the outlet.
3) further increase in oil production beyond this point (and most of the oil is indeed produced only after gas breakthrough in the low rate experiment) is due mainly to disconnected clusters of gas continuing to displace oil internally.
4) Once all isolated gas clusters join a cluster that is connected to the outlet port, or become connected to the outlet themselves, oil is no longer displaced and production stops.
5) the foregoing remarks may explain why high depletion rates result in high oil production — more bubbles are nucleated at high rates and this ensures that gas displaces oil from areas of the pore-space that would not be accessed via the sparse gas clusters that are characteristic of low rate depressurisation. In addition, bubbles grow competitively and at a slower rate during fast depletions and only interconnect when the overall gas saturation is relatively high.

The above picture of depressurisation in heavy oil is confirmed by our network simulations, as will be shown later.

Among additional factors that could affect oil production at the core scale, we note:
1) gravity: gas production can be accelerated and oil production slowed down by gravitational effects when gas accumulates at the top of a core [9].
2) heterogeneity: clearly this can be an important issue, as different areas of a core could have different nucleation characteristics and different capillary entry

characteristics. This could lead to differential gas liberation from different parts of a core [10].

It should be noted that these issues have not been addressed as part of the current study.

SET-UP OF THE NETWORK MODEL

A previously developed methodology [11] has been applied to anchor the pore network to the core. Two sets of mercury injection capillary pressure data (representative of different samples of the core) were provided by the experimentalists and matched in order to infer information about the pore size distribution and the connectivity of the system. Each data set represents different parts of the core.

The full results from the matching procedure are reported in Table 3 for both plugs. A power law pore size distribution has been assumed with exponent n and pore volumes are taken to be proportional to the capillary entry radius r raised to some power ν. Parameter combinations were derived via best matches to the experimentally-determined capillary pressure data. One of the main conclusions of the matching procedure was that the two samples appear to be differently connected with coordination numbers Z=6 and Z=4.9 respectively (a full discussion of the anchoring procedure, outlining its strengths and weaknesses, can be found in [11]).

THE DEPRESSURISATION NETWORK SIMULATOR

The pore scale network simulator developed here takes into account the pertinent physics of depressurisation; from the very nucleation of bubbles, to their growth by expansion and diffusion, and their subsequent coalescence and migration. We show that the growth of gas bubbles resembles a modified invasion percolation process, where each bubble can grow to a neighbouring pore if the relevant gas-liquid capillary pressure overcomes the capillary entry pressure of that pore.

The characteristics of the simulator have been presented elsewhere [8,12,13]: here we add a progressive nucleation algorithm and use it to match the productivities of core experiments. The algorithm nucleates bubbles at spatially random sites characterised by increased nucleation potential (either crevices containing pre-existing bubbles and/or chemical impurities). The model takes a positional information approach, whereby the degree of local supersaturation is taken into account when deciding if an embryonic bubble should form in a potential nucleation site. This is in agreement with some of the latest theories [14,15] regarding bubble nucleation in porous media, although there is still a lot of speculation on the real nature of the process. Nevertheless, the algorithm used here gives a qualitative idea of the bubble densities which can be expected to arise during a depletion experiment on the basis of the depletion rate and rock-fluid parameters. A full description of the progressive nucleation model can be found in [8].

HISTORY MATCHING

To match the experimental production data, we need to reproduce the key conditions of the core experiment at the level of network simulations. We believe that gas structures connected to the production port of the experimental apparatus are a major factor in determining the observed production profiles, and so the boundary conditions on our network model need to be consistent with this: hence, gas is allowed to escape from the network once connected to the outlet. This has been implemented by adding a buffer with large pores (larger than the largest pore present in the network), so that when gas connects to the outlet it no longer grows in the network (only disconnected clusters would continue to grow). This reflects the ideas previously expressed. All simulations have been run on networks of size 20X20X20 bonds with a buffer at the top (chamber of gas expansion) of dimensions 5X20X20 bonds.

Following the observations above we match the experimental data under the following assumptions:

1. the relevant features of the core experiment can be captured at the scale of a small network model;
2. the amount of oil produced reflects the gas saturation inside the system;
3. the overall effect of a connate water saturation is to effectively reduce the connectivity of the hydrocarbon network.

Whilst assumption (2) is reasonable in light of an earlier discussion in this paper, assumption (1) is a matter of some debate: a more detailed study should probably involve careful scaling-up of the network results via a laboratory-scale finite-difference simulator. Assumption (3) is reasonable and follows from the fact that water is not preferentially displaced by gas due to the typically high values of gas-water interfacial tension [8].

In Figure 2, a history match of gas saturations (relative to HCPV) is presented for the well connected, high permeability pore sample. The parameters used for the matching are presented in Table 4. By utilizing the progressive nucleation algorithm, different depletion rates naturally give rise to different bubble densities (without further tuning of the model). This is a classic example of the power of the network modeling approach, whereby several sensitivities can be undertaken using a model that has been suitably anchored using only a single experiment. It can be seen in Figure 2 that the overall production profiles are reproduced well up to the point of gas breakthrough (this is more evident in the high rate case, where gas breakthrough comes much later). We believe that differences observed after gas breakthrough could be due to scale effects and/or core-scale heterogeneity — if a core experiment could be run under the same conditions as our network simulation, one would not expect to observe continuous oil production throughout the experimental pressure range. However, further work might be required to improve the history match at low pressures.

RELATIVE PERMEABILITIES

We have seen how productivities have been matched using an unsteady-state approach: the network model was assumed to be positioned somewhere at the top of the core. The gas produced in this small network was then allowed to escape through the uppermost boundary which is consistent with the uppermost boundary of the core (outlet). We can now use the network model to calculate corresponding *steady*-state relative permeabilities if they exist (although it should be noted that the relative permeability concept is a little more complex than this in reality, as the gas is mainly in the form of disconnected slugs). In Figure 3 the relative permeabilities corresponding to the experimental history-match in Figure 2 are shown in linear and semi-log coordinates. The steady-state gas relative permeability becomes non-zero just at the end of the experiment for the high depletion rate, whilst it stays zero all the time at the lower depletion rate. This is primarily because a continuous, system-spanning gas cluster fails to form during the depletion. The very late appearance of a connected gas phase during the experiment (the point at which Krg first becomes non-zero) implies that any gas produced earlier would probably be the result of discontinuous gas slugs migrating independently upwards. Notice also, that the model predicts that steady-state oil relative permeablities would remain high at the end of the experiment and that substantial further oil production would still be possible via secondary gas injection. In future work, we hope to measure gas and oil fluxes directly in the buffer region in order to determine unsteady-state, anisotropic relative permeabilities —we believe that the traditional Darcian approach needs to be extended for depressurisation studies.

EXTRAPOLATION TO A LESS CONNECTED CASE

In order to highlight the important role played by pore connectivity during the depressurisation process, the same parameter set used for the history match of the well-connected experimental sample (Z=6) was applied to a poorly connected medium (Figure 4). The same cavity site distribution, critical supersaturation, IFT and diffusivity were chosen as before — only the coordination number was different (Z=3.6). This resulted in a marginal increase in the number of bubbles being nucleated than before (35 bubbles nucleated compared with 31 for the Z=6 case). Moreover, fewer oil-filled pores are present in the less connected system and the number of bubbles per unit volume of oil (i.e. bubble density) is consequently *much higher in the less connected system*. Overall, recovery was better in the poorly connected medium. The increase in bubble density is due to the fact that more areas of high supersaturation are produced in a poorly connected system and this will now be discussed in greater detail.

DISCUSSION ON CONNECTIVITY EFFECTS

Intuitive reasoning based upon percolation theory would lead one to the conclusion that a decrease in the connectivity of a system should lead to increased oil trapping after gas evolution (fewer escape routes are available to the displaced oil and the oil percolation threshold is higher in low connectivity systems). However, this topological trapping

effect is counterbalanced by the following, equally important, diffusion-related phenomenon.

Supersaturation is a function of both space and time: it increases *spatially* as we move towards oil pores which are far removed from equilibrated, gas-rich regions of the pore space; and it increases *temporally* in situations where diffusion is too slow to keep pace with depletion rate. Consequently, oil pores far away from gas pores become highly supersaturated during depressurisation experiments (especially at high depletion rates), and it becomes increasingly likely that such pores will nucleate additional embryonic bubbles. This is because diffusion pathways are, on average, longer for less connected systems and the gas flux between two pores decreases with increasing diffusion length as a consequence of Fick's first law,

$$j_{ij} = -\frac{D(C_j - C_i)}{L} \tag{1}$$

where j_{ij} is the mass flux from pore i to j, C_j the gas concentration in pore i, C_j the gas concentration in pore j, D the diffusion coefficient and L the length of the diffusion pathway as specified above. This is shown schematically in Figure 5. It follows that, although low connectivity enhances oil trapping, it also increases bubble nucleation density which, in turn, allows additional oil to be displaced by bubbles nucleating in areas of pore space that would remain bubble-free in a highly connected medium. It is impossible to predict *a priori* which of these two competing effects will dominate a particular depletion experiment, and so it is clearly possible to conceive of cases where poor connectivity is accompanied by good recovery (and, conversely, cases where a high bubble density could be accompanied by poor recovery).

Figure 6 shows the effect of connectivity upon supersaturation at different depletion rates. The term supersaturation is used here to denote how far the gas-oil system is from equilibrium: in other words if the average content of dissolved gas in oil is higher than PVT relations would predict (at any given pressure) then the system would be classed as being supersaturated. Here, a single bubble has been nucleated at a critical supersaturation of 40 psi in the centre of a 15X15X15 network (more than 10,000 pores). Further nucleation has been deliberately suppressed, as the main point of interest here is to determine information relating to the evolution of *average* supersaturation in the network. The average supersaturation is computed by tracking pore-by-pore the content of dissolved gas in oil and comparing it to the relative PVT value. From Figure 6, we can deduce that supersaturation increases not only with depletion rate (which is well known) but also increases with decreasing connectivity (represented here by the coordination number Z). This is an important result — although connectivity effects can be considered negligible at reservoir depletion rates, they become increasingly dominant in high-rate laboratory experiments and may lead to erroneous estimates of critical gas saturation and hydrocarbon recovery (notice also that PVT assumes everything is in

equilibrium and the results presented here show that this may not necessarily be the case, particularly at laboratory depletion rates).

CONCLUSIONS

The depressurisation network simulator has proved to be a very useful tool in understanding the pore-scale mechanisms governing the solution gas drive process. Its predictive potential has been enhanced in the present work by adding a progressive nucleation algorithm, which gives new insight into many of the issues related to nucleation in porous media. In particular, practical problems of interest to the reservoir engineer have been addressed, such as critical gas saturation, production profiles, and relative permeabilities at different depletion rates.

The pore-scale process simulator was used here to interpret the underlying dynamic processes that characterise a long-core heavy oil depletion experiment. This was achieved by direct matching of experimental gas and oil production profiles under different depletion rates. In order to achieve this, we needed to reproduce the key conditions of the core experiment at the level of network simulations. We believe that gas structures connected to the production port of the experimental apparatus were a major factor in determining the observed production profiles, and so the boundary conditions on our network model were designed to be consistent with this. Once this condition had been taken into account, successful history matches were achieved for both the high and low rate experiments. It transpired that the relevant tool for history-matching core experiments was the crevice size distribution (or, more generally, the "nucleation potential" distribution).

Whilst productivities were matched using an unsteady-state approach, with the network assumed to be positioned at the top of the core and gas escaping into a buffer, a set of *steady*-state relative permeabilities were also calculated. The model predicted that oil relative permeablities would remain high at the end of the experiment and that substantial further oil production would still be possible via secondary gas injection. To further extend our relative permeability interpretation, however, it is of central importance to understand the link between the network scale and the core scale. Matching the productivities has suggested that during the depletion experiment there are regions of the core characterised by different gas saturations. Hence, as far as network modeling is concerned, any estimate of relative permeability should be a function of the precise position in space that the small network has inside the core. This issue will be more fully addressed as part of future work.

Finally, in order to highlight the important role played by pore connectivity during the depressurisation process, the same parameter set used for the history match of the well-connected experimental sample (Z=6) was applied to a poorly connected system (Z=3.6). It was found that, although low connectivity enhanced oil trapping, it also led to an increased bubble nucleation density which, in turn, allowed additional oil to be displaced by bubbles nucleating in areas of pore space that would have remained bubble-free in a

highly connected medium. It is therefore possible to conceive of counterintuitive cases where a high bubble density could be accompanied by poor recovery or poor connectivity accompanied by good recovery.

ACKNOWLEDGEMENTS

The authors would like to thank Total for financial and technical assistance throughout the course of this study.

REFERENCES

1. Smith, G. E.: "Fluid flow and sand production in heavy oil reservoirs under solution gas drive", SPE 15094, 29-40, 1986.
2. Dusseault, M. B. and El-Sayed, S. "Heavy-oil production enhancement by encouraging sand production",SPE 59276, 2000.
3. Maini, B.: "Foamy oil flow in primary production of heavy oil under solution gas drive", SPE 56541, 1999.
4. Mastmann, M., Moustakis, M. L. and Bennion D. B.: "Predicting foamy oil recovery", SPE 68860, 2001.
5. Bora, R., Maini, B. B. and Chakma, A.: " Flow visualization studies of solution gas drive process in heavy oil reservoirs with a glass micromodel", SPE Reservoir Eval. & Eng. 3 (3), 224-229, 2000.
6. Akin, S. and Kovscek, R.: "Heavy oil solution gas drive: a laboratory study", Journal of Petroleum Science and Engineering", 35, 33-48, 2002.
7. Bayon, Y., Cordelier, Ph., Nectoux, A.: "A New Methodology to match Heavy-Oil Long Core Primary Depletion Experiments:" SPE 75133, SPE/DOE symposium on Improved Oil Recovery, Tulsa, USA, April 2002
8. Bondino, I., McDougall, S., R. and Hamon, G.: "Pore network modeling of heavy oil depressurization: a parametric study of factors affecting critical gas saturation and 3-phase relative permeabilities", SPE 78976, 2002.
9. Urgelli, D., Durandeu, M., Foucault, H. and Besnie, J-F.: "Investigation of foamy oil effect from laboratory experiments", SPE 54083, 1999.
10. Andarcia, L., Kamp, A., M. and Vaca, P.: "Heavy oil solution gas drive in the Venezuelan Orinoco Belt: laboratory experiments and field simulations", SPE 69715, 2001.
11. McDougall, S., R., Cruickshank, J. and Sorbie, K., S.: "Anchoring methodologies for pore-scale network models: application to relative permeability and capillary pressure prediction", paper SCA 2001-15, presented at the 2001 SCA
12. McDougall, S. R. and Mackay, E. J.: "The impact of pressure-dependent interfacial tension and buoyancy forces upon pressure depletion in virgin hydrocarbon reservoirs", Trans IchemE, Vol. 76, Part A, Jul. 1998.

13. McDougall, S. R. and Sorbie, K. S.: "Estimation of critical gas saturation during pressure depletion in virgin and waterflooded reservoirs", Petroleum Geoscience, Vol. 5, 229-233, 1999.
14. Jones, S.F., Evans G.M. and Galvin K.P.: "Bubble nucleation from gas cavities-a review", Advances in colloid and interface science, 80, 27-50, 1999.
15. Tsimpanogiannis, I. N. and Yortsos, Y. C.: "An Effective Continuum Model for the Liquid-To-Gas Phase Change in a Porous Medium Driven by Solute Diffusion: I. Constant Pressure Decline Rates", SPE 71502, 2001.

Table 1. Core properties for the heavy oil long-core experiment

Length (cm)	90.90
Diameter (cm)	4.99
Porosity (average)	0.216
Permeability to water (mD)	630
Swi (%)	18.7
Water salinity (g/l - NaCl)	16
vertical	vertical
Net confining pressure	100 bars
Temperature	50°C
Pore volume at reservoir conditions	383.3 cm3
Brine permeability at reservoir conditions	630 mD
Initial Brine volume	71.6 cm3

Table 2. Fluid properties for the heavy oil long-core experiment

Gas density (at surface conditions)	0.78 kg/m3
Oil density (at surface conditions)	984 kg/m3
Oil bubble point pressure	754 psi (51.3 atm)
Gas-Oil interfacial tension	22.0-25.0 mN/m
Water-oil interfacial tension	14.0-16.0 mN/m

Table 3. Results from the anchoring procedure for two different capillary pressure mercury injection data sets

High permeability sample (K=884 mD)	
Rx maximum radius	$25X10^{-6}$ m
Rm minimum radius	$5X10^{-6}$ m
N, psd exponent	-1.1
ν, volume exponent	2
Z, co-ordination number	6
pore length	$88X10^{-6}$ m
porosity	0.216

Low permeability sample (K=354 mD)	
Rx maximum radius	$21X10^{-6}$ m
Rm minimum radius	$4.75X10^{-6}$ m
N, psd exponent	-1.8
ν, volume exponent	2
Z, co-ordination number	4.9
pore length	$88X10^{-6}$ m
porosity	0.216

Table 4. Parameters and bubble densities for the history matching of Figure 2

Rayleigh Cavity Site Distribution (1crevice per 150 pores)	Range (m): $4*10^{-8}$ to $10*10^{-8}$
Critical supersaturation	90 psi
IFT	0.022 N/m
Diffusivity	$2.0X10^{-6}$ m^2 /day
N bubbles low rate	9 (1 bub per 2710 pores)
N bubbles high rate	31 (1 bub per 790 pores)

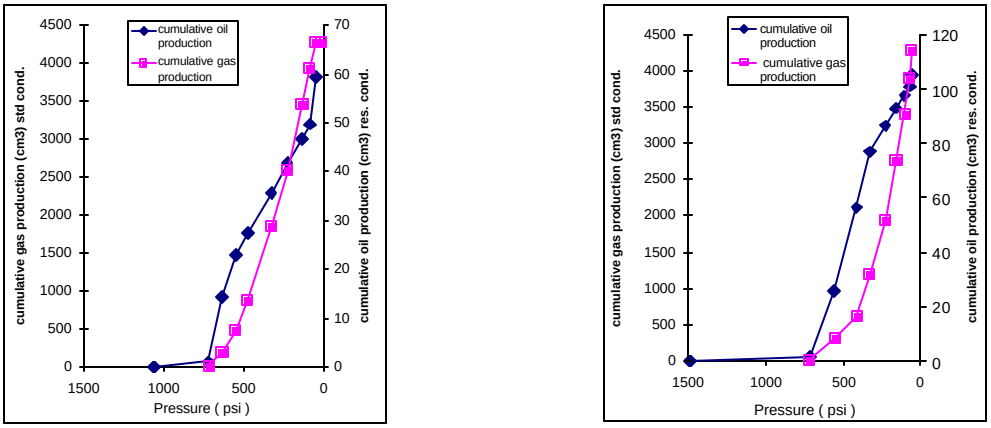

(a) (b)

Figure 1. Cumulative gas and oil production for the lower rate (a) 9 psi/day, and for the higher rate (b) (100 psi/day) experiments

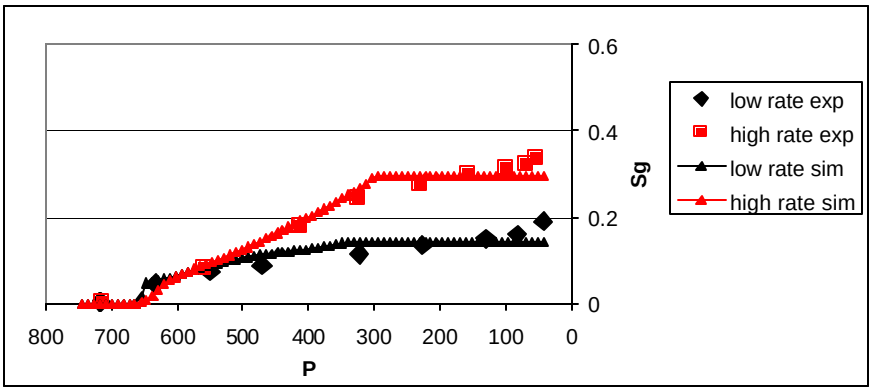

Figure 2. History matching of gas saturations inside the core via network simulations for the well connected highly permeable case, Z=6 (simulations on 20X20X20 networks)

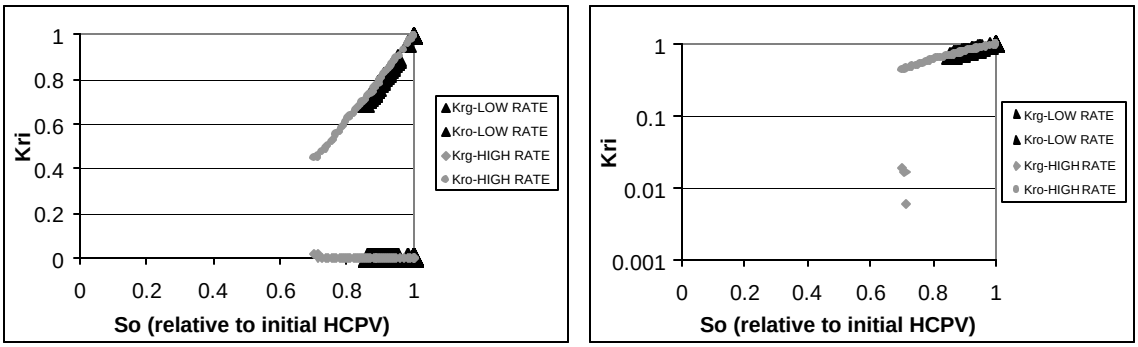

Figure 3. Relative permeabilities for the history matching in Figure 2 on both linear (a) and semi-log (b) scales

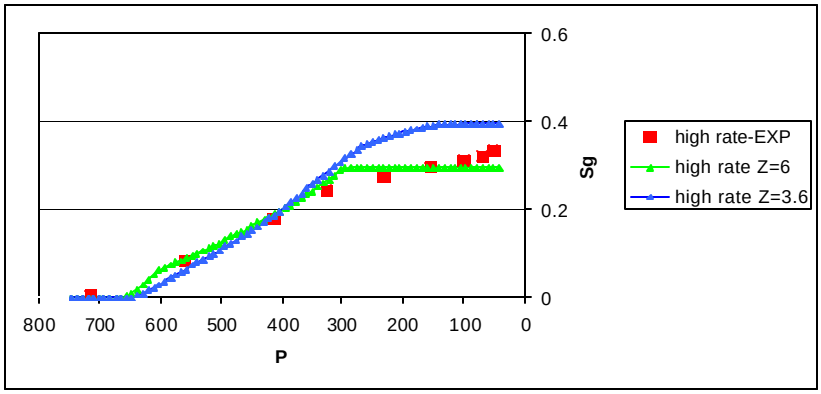

Figure 4. Extrapolation to the less connected system with coordination number Z=3.6 of the history matching parameters of Table 4 (depletion rate selected: 100 psi/day)

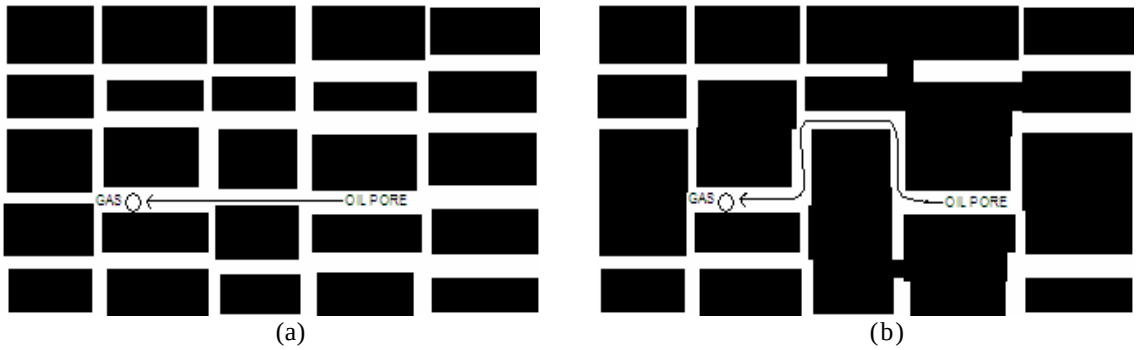

Figure 5. In the well connected system (a) diffusion acts more effectively in transporting dissolved gas from the oil pore into the gas bubble. In (b) the path of diffusion is more tortuous and the pore will become highly supersaturated at the point in the depletion

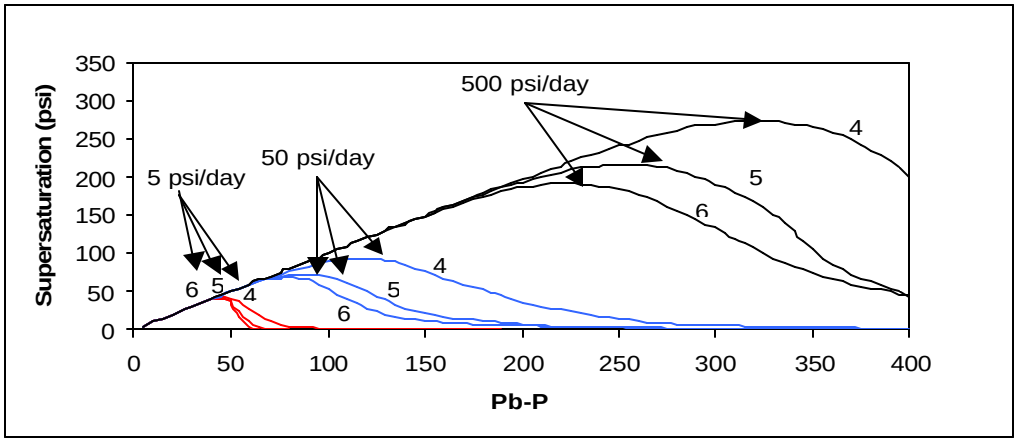

Figure 6. Supersaturation Vs depletion pressure for different depletion rates and coordination numbers